Fault Detection of Rotor Bars in Inverter-Fed Induction Motors Based on Current Signature Analysis Technique

Tomoyuki Iwawaki,[1*] Makoto Kanemaru,[1] Yuto Yasuhara,[2] and Toshihiko Miyauchi[2]

[1]*Mitsubishi Electric Corporation, Advanced Technology R&D Center, Amagasaki, Hyogo, 661-8661, Japan*
[*]*Corresponding author: Iwawaki.Tomoyuki@dh.MitsubishiElectric.co.jp*

[2]*Mitsubishi Electric Corporation, Power Distribution Systems Center, Marugame, Kagawa, 763-8516, Japan*

ABSTRACT

Induction motors, which are one key piece of equipment for power plants, waterworks facilities, and factories, must be maintained appropriately for reliable operation. A motor current signature analysis (MCSA) technique, which monitors and detects problems in motors and diagnoses devices, has already been marketed by some companies. Recently, applications of inverter-fed motors have increased for greater energy conservation. However, a fault-detection method in inverter-fed motors has been inadequately studied despite the risk of misdetection due to inverter noise. This paper shows our results that detected a broken rotor bar in an inverter-fed motor based on a MCSA technique. An abnormal motor with a broken rotor bar and a normal motor are driven by an inverter. The current supplied to both motors is measured and the frequency spectra results are compared. In the measurements, the inverter's drive frequency is varied from 120 to 10 Hz in 10 Hz increments. In each drive frequency, the slip is varied in a range of 0-5% by adjusting the load connected to the motor. The results of comparing the current spectra show significant reinforcement of the signal intensities in abnormal motors. Some signals are reinforced by both inverter noise and a component that originated in the broken bar. The superposition that may lead to a misdiagnosis in inverter-fed motors is avoided by identifying the normal spectrum shapes of the target equipment in advance.

1. INTRODUCTION

The motor current signature analysis (MCSA) technique detects abnormalities in an induction motor (IM) and its load by measuring the voltage and current supplied to it [1, 2]. This technique enables low-cost and constant monitoring of IM health. Diagnosis devices have already been marketed by some companies and implemented on power plants, waterworks facilities, and factories. Recently, applications of inverter-fed motors have increased for more energy conservation. However, this technique struggles to accurately detect abnormalities when the IMs are driven by inverters due to the superposition of the inverter noises generated in the range of the current spectrum for detecting abnormalities [3, 4]. As a first step to tackle this problem, we previously studied the generation of inverter noise by a theoretical approach that predicted noise frequency that depends on the inverter's setting conditions [3]. In this paper, we extend the previous study and show results that detected a broken rotor bar in an IM actually driven by a V/f-controlled pulse width modulated (PWM) inverter. The broken rotor bar is one of the major failure modes in IM.

2. FREQUENCIES OF BROKEN ROTOR BAR AND INVERTER NOISE

For conducting an MSCA, the time waveform of the current supplied to an IM has to be converted into a frequency spectrum by frequency analysis, such as Fast Fourier Transform (FFT). Diagnosis devices judge the IM health from the peak frequencies and the signal intensities in the current spectrum. The characteristic frequencies that indicate abnormalities differ depending on the cause of the occurrence. When an IM is driven by an inverter, in addition to the characteristic frequencies, the spectral peaks caused by the inverter appear as noise in the frequency spectrum. The frequencies of these peaks depend on the frequencies of the power supplied to the inverter and the IM in addition to the carrier and the sampling frequencies in the inverter.

2.1. Broken rotor bar frequency

A rotor bar is stressed by a large starting current and centrifugal force due to rotation, causing such damage as cracks and breaks. When a drive current of frequency f_0 flows in the stator, current of frequency sf_0 is induced in the rotor with slip s. When a rotor bar is damaged, current of frequency $-sf_0$ (i.e., a negative sequence component) is produced in the rotor. This component induces a current of frequency $(1-2s)f_0$ into the stator. The frequency $-sf_0$ current produces a torque ripple at frequency $2sf_0$ that leads to the following current of rotor bar frequency f_{rb} in the stator [5].

$$f_{rb} = (1 \pm 2s)f_0 \quad (1)$$

The rotor bar frequencies appear as a sideband centered on drive frequency f_0. In this paper, the components of $(1+2s)f_0$ and $(1-2s)f_0$ are describe as an upper sideband (USB) and a lower sideband (LSB). When a rotor bar is seriously damaged, the current of frequency $-sf_0$ in the rotor is increased, which significantly reinforces the signal intensities at the rotor bar frequencies in the spectrum. A rotor bar abnormality is diagnosed by confirming the reinforcement.

2.2. Inverter noise frequency

Assuming a situation where the rotor bar frequencies are up to several hundred Hz, inverter noises are mainly a problem in the low frequency range [3]. When the PWM inverter generates a rectangular voltage, if carrier frequency f_c and sampling frequency f_s are not multiples of drive frequency f_0, the following frequencies of noise F_{pwm} are produced.

$$F_{pwm} = i\mathrm{GCD}(f_0, f_s, f_c) \quad (2)$$

Here, GCD is the greatest common divisor and i is a positive integer. For example, when f_0 = 60 Hz, f_s = 8 kHz, f_c = 2 kHz, GCD (f_0, f_s, f_c) is 20 Hz and F_{pwm} are 20 Hz, 40 Hz, 60 Hz, and so on. If carrier frequency f_c and sampling frequency f_s are multiples of drive frequency f_0, the frequencies of the noise are the harmonics kf_0 of driving frequency f_0 with k as a positive integer.

In addition, the converter inside the inverter produces noise of frequency F_v in the process of generating DC voltage.

$$F_v = |mf_{ac} \pm nf_0| \quad (3)$$

Here, m and n are positive integers, and f_{ac} is the frequency of the power supplied to the inverter. For example, when f_0 = 60 Hz and f_{ac} = 50 Hz, the F_v are 10 Hz, 20 Hz, 30 Hz, and so on.

Since these noises are produced in the low frequency range, they may overlap with the rotor bar frequencies. Furthermore, a lot of noise is produced that cannot be expressed by these formulas. To diagnose the IM health, such noises must be appropriately dealt with.

3. MEASUREMENT

3.1. Configuration

Figure 1 shows the measurement configuration. First, the power is supplied from the distribution board to the AC power supply, which provides power to the PWM inverter with a frequency of 60 Hz and a voltage of 200 V. The PWM inverter conducts the V/f control to the three-phase standard IM whose rated output is 0.75 kW with two pole pairs. The drive frequency is set from 120 to 10 Hz in 10 Hz increments. The IM is connected to the torque detector (KYOWA, TP-10kMCB) following the brake, which adjusts the load applied to the IM to measure the dependence of the rotor bar frequency against a slip. Here, the load is varied from 0% to 120% of the rated load. The current supplied from the inverter to the IM is measured by a current probe (YOKOGAWA, 701933) connected to a memory HiCorder (HIOKI, 8875). The speedometer (ONOSOKKI, HT-4200) is installed at the connection between the IM and the torque detector to measure the IM's rotational speed. Under this measurement configuration, an IM with one broken rotor bar (Fig. 2) is driven to detect the signals of the broken rotor bar frequencies. At the measurement, a current of another normal IM is also measured at the same configuration for a comparison.

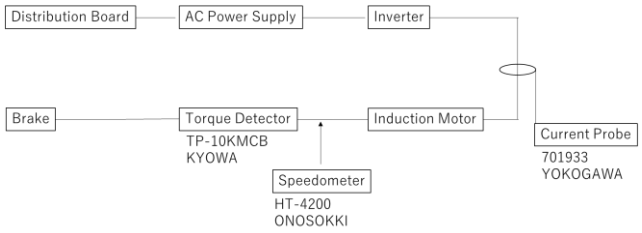

Fig. 1. Measurement configuration.

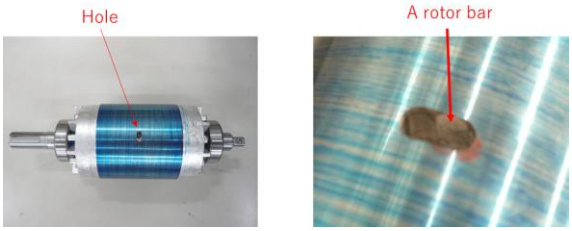

Fig. 2. Rotor with one broken bar.

3.2. Evaluation

A Fast Fourier Transform with a Hanning window function converts the time waveform of the current stored at the memory HiCoder to the frequency spectrum. As shown in Eq. (1), a slip is necessary to specify the rotor bar frequency in the frequency spectrum. Slip s is calculated by Eq. (4) using rotation speed N_r measured by the speedometer and synchronous speed N_0.

$$s = \frac{N_0 - N_r}{N_0} \quad (4)$$

The frequency components of the rotor bar are specified in the acquired frequency spectrum (Eqs. (1) and (4)). For example, Fig. 3 shows the frequency spectra acquired from the abnormal IM as a red solid line and the normal one as a black dashed line. The figure also shows the rotor bar frequencies for the health of each motor. Both drive frequencies are identical at 60 Hz, and their rotation speeds are 1762 rpm at the abnormal motor and 1765 at the normal one. The rotor bar frequencies calculated with Eqs. (1) and (4) are 57.47 Hz (LSB) and 62.53 Hz (USB) at the abnormal motor and 57.67 Hz (LSB) and 62.33 Hz (USB) at the normal one. The spectral peaks with the highest intensity within 0.2 Hz from these theoretical values are defined as the rotor bar frequencies. The signal intensities are -39.88 dB (LSB) and -39.33 dB (USB) at the abnormal motor and -59.19 dB (LSB)

and -59.11 dB (USB) at the normal one. The comparison confirms that the signal intensities at the rotor bar frequencies are reinforced due to the broken rotor bar.

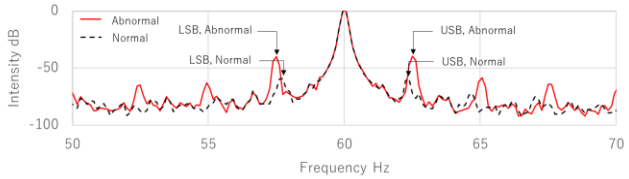

Fig. 3. Frequency spectra and sidebands of rotor bar frequencies at drive frequency of 60 Hz. Red solid and black dashed lines indicate spectra of abnormal and normal IMs.

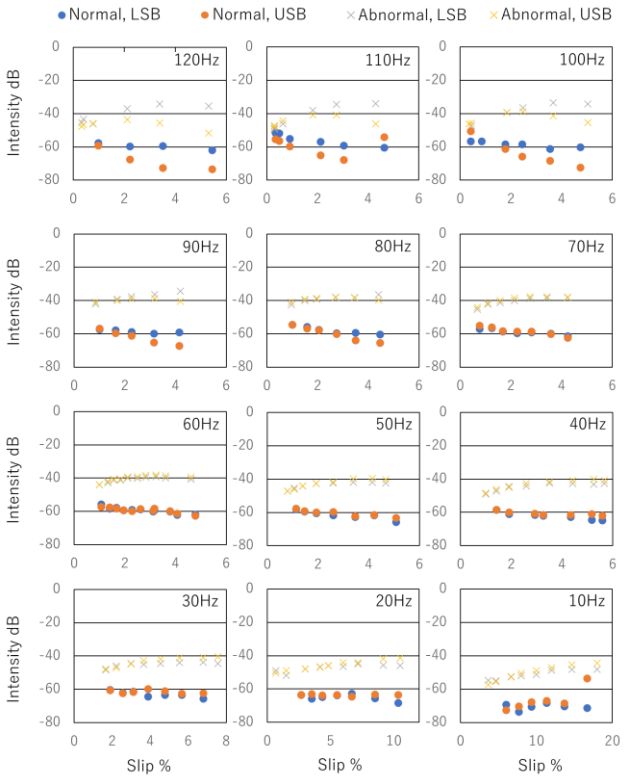

Fig. 4. Dependences of signal intensity against slip in each drive frequency from 120 to 10 Hz. Each graph indicates signal intensities of LSB and USB at abnormal and normal IMs.

Figure 4 shows the dependences of the signal intensity against slips in each drive frequency from 120 to 10 Hz in 10 Hz increments. The graphs of each drive frequency show the signal intensities of LSB and USB at the abnormal and normal IMs. All graphs indicate that the signal intensity at the abnormal IM is significantly reinforced compared with that at the normal one. The reinforcement detects the damage of the rotor bar in the inverter-fed IM. However, as indicated at a USB intensity of a 4.6% slip at the normal IM, some intensities are much more reinforced, judging from the overall dependency trend of the intensity against slips. These excess reinforcements occur due to superposition of the rotor bar frequency and the inverter noise. Fig. 5 shows the frequency spectra of 4.6%, 3.0% and 2.1% slip and of the USB positions. Here each intensity is adjusted based on the floor noise. A spectrum peak at 120 Hz, which was considered with the inverter noise from Eqs. (2) and (3), was confirmed at each frequency. We also confirmed that the USB approaches the inverter noise as the slip increases and is overlapped at a 4.6% slip. Thus, the USB intensity of a 4.6% slip at a normal IM is much more reinforced. The superposition of the rotor bar frequency and inverter noise should be avoided to avoid misdiagnosis.

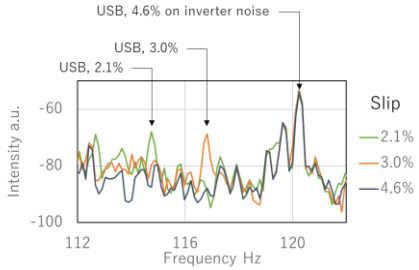

Fig. 5. Frequency spectra of 4.6%, 3.0%, and 2.1% slip at normal IM with each USB.

3.3. Avoiding superposition of rotor bar frequency and inverter noise

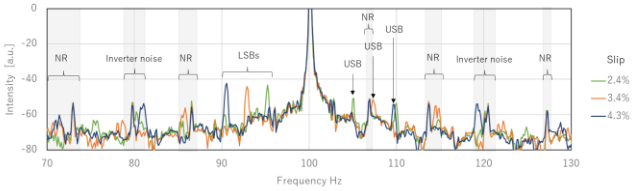

Fig. 6. Frequency spectra of 2.4%, 3.4% and 4.3% slips at normal IM driven 100 Hz. Hatched ranges cannot be utilized for diagnosis.

Figure 6 shows the frequency spectra of 2.4%, 3.4% and 4.3% slips at a normal IM driven at 100 Hz. Here each intensity is adjusted based on the floor noise. The frequency spectra include the rotor bar frequencies, LSBs and USBs, which depend on the slip as shown by Eq. (1). The inverter noises calculated from Eqs. (2) and (3) are confirmed at 80 and 120 Hz. Because the frequencies of the inverter noise are independent of the load in principle, they exist around the calculated frequencies in similar spectral shapes. In addition to these noises, noisy ranges (NRs) were confirmed at around 70, 106, 115, and 128 Hz. Even if the slip varied, the spectral shapes are almost the same due to the same condition of inverter, and the intensities remain high in each NR. As described at Fig. 5, when the rotor bar frequency overlaps with the noise in NR, the intensity is much more reinforced. Fig. 6 indicates an NR around 106 Hz near the USB of a 3.4% slip. This USB barely avoids superposition with the noise in NR. However, this situation suffers from a high risk that the

USB frequency will overlap with the noise in NR due to a slight fluctuation of the load connected to the IM. To avoid the risk of superposition in this case, the LSB intensities are utilized for diagnosis because NR doesn't exist in the range of the LSBs.

NR is generated almost independently of the load, as with inverter noise. Therefore, by learning the spectral shapes of the equipment before performing a health diagnosis and identifying the noise features in advance that assigns the ranges cannot be utilized to diagnosis, we can detect abnormality in the rotor bar of the inverter-fed IM.

4. CONCLUSION

Regarding a broken rotor bar in an induction motor (IM) that was V/f controlled by a pulse width modulated (PWM) inverter, we confirmed using a motor current signature analysis (MCSA) technique that the signal intensity of the characteristic frequency increased significantly at an IM with a broken rotor bar. We also confirmed that some rotor bar frequency intensities were much more reinforced due to superposition with noise. Superposition may lead to misdiagnosis of the diagnosis device. Since the noise's spectral shapes are almost the same against the load, this possibility can be avoided by learning the characteristics of the equipment in advance at the implementation.

REFERENCES

1. M.E.H. Benbouzid (2000). *A Review of Induction Motors Signature Analysis as a Medium for Faults Detection*, IEEE Transactions on Industrial Electronics, vol. 47, no. 5, pp. 984-993.
2. S. Nandi, H. A. Toliyat, & X. LiFerrell (2005). *Condition Monitoring and Fault Diagnosis of Electrical Motors—A Review*, IEEE Transactions on Energy Conversion, vol. 20, no. 4, pp. 719-729.
3. M. Miyoshi, Chen, K. Hirakida, S. Sano, R. Sugawara, M. Kanemaru, & T. Miyauchi (2020). *Current Signature Analysis of Induction Motor Avoiding the Effect of Time Harmonics from Inverter.* Proceedings of IEEJ Seminars in MD-20-102-155/RM-20-095-148/LD-20-045-098, pp. 185-188.
4. M. Kanemaru, T. Ohkubo, S. Sano, A. Satake, & S. Terashimara (2019). *Investigating Current and Radial Shaft Displacement of Induction Motor Driven by Pulse-Width Modulation Inverter for Bearing Fault Detection*. Proceedings of IEEE 12th International Symposium on Diagnostics for Electrical Machines, Power Electrics and Drives (SDEMPED), pp. 377-383.
5. F. Filippetti, G. Franceschini, C. Tassoni, & P. Vas (1998). *AI Techniques in Induction Machines Diagnosis Including the Speed Ripple Effect*. IEEE Transactions on Industry Applications, vol. 34, no. 1, pp. 98-108.